Evaluation of interparticle interactions between magnetic nanoparticles using first order reversal curves and Weiss temperature

Journal of Physics Communications

OPEN ACCESS

RECEIVED
12 January 2021

REVISED
7 March 2021

ACCEPTED FOR PUBLICATION
12 March 2021

PUBLISHED
6 April 2021

PAPER

Evaluation of interparticle interactions between magnetic nanoparticles using first order reversal curves and Weiss temperature

H Mamiya[1], **I Furukawa**[2], **J L Cuya Huaman**[2], **K Suzuki**[2], **H Miyamura**[2] and **B Jeyadevan**[2]

[1] National Institute for Materials Science, Tsukuba, Ibaraki 305, Japan
[2] The University of Shiga Prefecture, Hikone, Shiga 522-8533, Japan

E-mail: MAMIYA.Hiroaki@nims.go.jp

Keywords: superspin-glass, fine particle, cooperative phenomena

Abstract

Two conventional methods for evaluating interparticle magnetic interactions are applied to magnetic nanoparticle assemblies with various interparticle distances that are controlled by a silica coating. According to Weiss temperatures derived from superparamagnetic response analysis, the mean values of the interparticle magnetic interactions are relatively small and seem to be independent of the interparticle distance. The interaction fields in the first-order reversal curve diagram for narrow interparticle distances are widely distributed. However, the interaction fields disappear when the interparticle distance is sufficiently large. Analysis of these two contrasting results indicates that ferromagnetic-like and antiferromagnetic-like magnetic couplings coexist and cancel each other, as in atomic spin glasses.

1. Introduction

Recently, magnetic nanoparticles have attracted significant attention for their excellent potential for applications in magnetic recording sensors [1, 2], magnetic refrigeration [3], and biomedical applications [4]. However, many issues remain to be solved regarding the design of magnetic nanoparticle assemblies for each application. In particular, there is little consensus regarding the effects of dipole interactions between nanoparticles, even though they are expected to induce useful cooperative magnetic responses [5, 6]. For single-domain magnetic nanoparticles with superspins $\mu\,(=(\pi/6)d^3M_0)$, the typical magnitude of dipolar interactions can be expressed as $\frac{\mu_0\mu^2}{2\pi r^3}$, where d is the diameter of the nanoparticle, M_0 is the spontaneous magnetisation, and r is the distance between nanoparticles. In other words, the amplitude of interactions can be controlled by varying r. Therefore, many efforts have been made to prepare nanoparticles with various r values by changing the particle number density or controlling the nonmagnetic layer thickness t between nanoparticles [7–13]. However, little attention has been devoted to the experimental evaluation of actual interparticle interaction strengths in such samples. In studies on randomly assembled nanoparticles, mixtures of ferromagnetic-like and antiferromagnetic-like interparticle interactions are assumed. Based on this assumption, superspin glasses have been intensively discussed in terms of their intriguing collective phenomena for decades, similar to atomic spin glasses. However, the mixture of interparticle interactions has never been experimentally confirmed [5–13]. In this study, two conventional evaluation methods, namely first-order reversal curve (FORC) analysis [14–16], which is often employed in applied magnetics, and Curie-Weiss law fitting, which is used in fundamental magnetism, were applied to nonmagnetic-layer thickness-controlled magnetic nanoparticle assemblies. The actual probability distributions of ferromagnetic-like and antiferromagnetic-like interparticle interaction strengths were investigated.

2. Experiments

Magnetite nanoparticles were synthesised as follows. First, 11.0 mmol of goethite (FeO(OH)) was dissolved in 31.7 ml of 1-octadecene. Next, 14.1 ml of oleic acid was added and the solution was heated at 393 K for 1 h and at

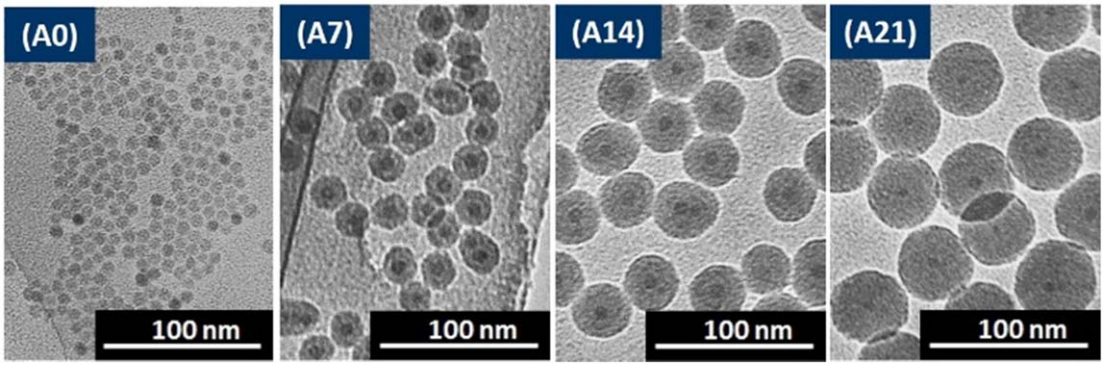

Figure 1. TEM images of magnetite nanoparticles in samples A0, A7, A14, and A21.

590 K for 2 h. The resulting black powder was washed several times to remove excess surfactants and solvents. X-ray diffractometry revealed that the powder had a spinel-type structure. Magnetometry indicated that M_0 at 2.0 K is 53 Am^2/kg. This magnitude of M_0 is roughly consistent with the values previously reported for iron oxide magnetic nanoparticles [17, 18], although it is smaller than the values obtained for bulk magnetite or maghemite. This study aimed to evaluate interparticle interactions, so the origin of the relatively small M_0 value is left unexplored for following studies.

Next, coating with a silica shell [19] was conducted as follows. Igepal CO-520 was dispersed in cyclohexane and sonicated. Then, the powder synthesised above was added to the solution under continuous stirring. Subsequently, 1.6, 1.6, and 3.2 ml of ammonium hydroxide and 1.12, 2.24, and 4.43 ml of tetraethyl orthosilicate were added to generate three different shell thicknesses. Transmission electron microscopy (TEM) revealed that the magnetite cores with an average diameter d of 7.8 nm were well coated with silica shells with thicknesses t of 6.5, 13.7, and 20.8 nm for samples A7, A14, and A21, respectively, as shown in figure 1. The nanoparticles before silica coating in sample A0 have a surfactant layer with $t = 1 - 2$ nm. Therefore, we succeeded in controlling the interparticle distance.

The magnetisation M of all samples was measured under the following thermal and field conidtions using a superconducting quantum interference device magnetometer (MPMS, Quantum Design). Zero-field-cooled magnetisation M_{ZFC} was measured under heating in a magnetic field H of 0.8 kA m^{-1} after zero-field cooling to 2.0 K, whereas field-cooled magnetisation M_{FC} was measured under cooling in a magnetic field H of 0.8 kA m^{-1}. The measurements of FORC were performed as follows. From a positive saturation state at an H values of 0.8 MA/m, H was decreased to a reversal field H_r. A partial hysteresis curve $M(H, H_r)$ was then measured as H increased from H_r back to saturation. This measurement procedure was repeated for several different H_r values.

3. Results and discussion

Figure 2 presents the temperature dependencies of M_{ZFC} and M_{FC}. As the temperature T increases, M_{ZFC} first increases, then peaks at T_m, and finally decreases. M_{FC} is almost the same as M_{ZFC} in the high-temperature range of $T \gg T_m$, whereas M_{FC} branches off from M_{ZFC} at $T < T_m$. These results have been conventionally interpreted as follows. The system is equilibrated by the thermal fluctuation of μ at $T \gg T_m$. In contrast, magnetic hysteresis occurs based on the suppression of fluctuations at $T < T_m$. The boundary temperature indicated by T_m, which is the so-called blocking temperature or freezing temperature, is reduced with an increasing coating thickness t, as shown in the inset in figure 2. This type of variation in T_m with a changing t has been attributed to the effects of interparticle magnetic interactions because the magnetic properties of individual nanoparticles should be invariant with t [5–10]. However, previous studies have not contained experimental evaluations of interparticle interaction strengths. Therefore, detailed discussion remains difficult. For this reason, two evaluation methods of FORC analysis and Curie-Weiss law fitting were applied in this study.

In the paramagnetic phases of atomic spin systems, the magnetisation at small H values is given by the Curie-Weiss law as follows:

$$M = \frac{n\mu_0\mu^2}{3k_B(T - T_w)}H = \frac{M_s\mu_0\mu}{3k_B(T - T_w)}H, \quad (1)$$

where n is the number density of magnetic moments μ, k_B is the Boltzmann constant, T_w is the Weiss temperature, and M_s is the saturation magnetisation. Figure 3 presents the temperature dependence of M_s/M, where the magnitude of M at 0.4 MA/m and 2.0 K is assumed to be M_s. One can see that M_s/M is approximately

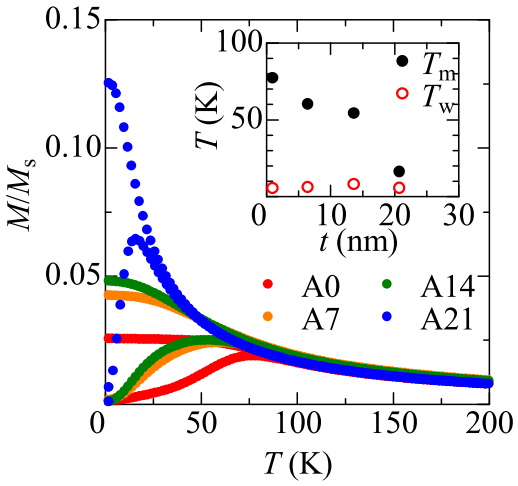

Figure 2. Temperature dependencies of M_{ZFC} and M_{FC} normalised by M_s. The inset shows the variation in T_m and T_w for various nonmagnetic silica-layer thicknesses t.

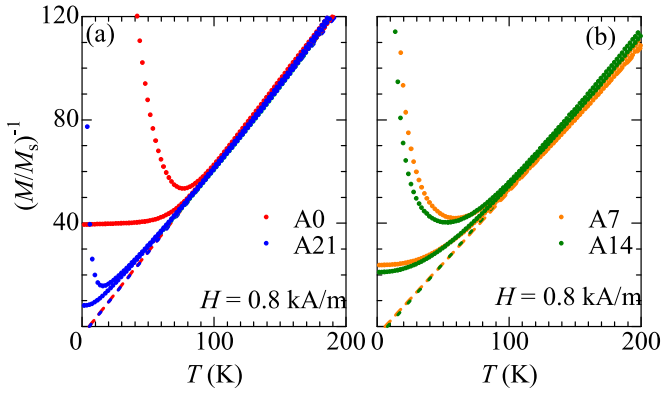

Figure 3. Temperature dependencies of the reciprocals of M_{ZFC} and M_{FC} normalised by M_s for (a) samples A0 and A21, and (b) samples A7 and A14.

proportional to T in the anhysteretic regime at $T \gg T_m$. Based on the slopes of the fitting lines, the magnitudes of μ can be roughly estimated to be $7 \times 10^3\ \mu_B$ for A0 and A21, and $8 \times 10^3\ \mu_B$ for A7 and A14. These values correspond to the total magnetic moments contained in each iron oxide nanoparticle with a size of 8 nm at an M_0 of 53 $Am^2\ kg^{-1}$. This size is consistent with the diameters observed via TEM. Therefore, we can confirm that collinearly aligned spins in each nanoparticle thermally fluctuate in the form of superspins $\boldsymbol{\mu}$. In contrast, the values of T_w estimated from the T-axis intercepts are less than 10 K and are almost independent of t, as shown in the inset in figure 2. In the molecular field approximation, T_w is expressed as $\alpha_0 M_s \mu / 3k_B$. Therefore, αM_s can be estimated to be less than 5 kA m^{-1}, regardless of t, where α is the molecular field coefficient. The magnitude and t-dependence of T_w contrast with those of T_m. Therefore, one may doubt the explanation above that the elevation of T_m is caused by interparticle interactions.

We turn to FORC analysis to resolve this conflict. To avoid the influence of thermal fluctuations, the FORC curves at 2.0 K, which is much lower than T_m, were examined, where each nanoparticle with a switching field of H_{sw} was assumed to be under a constant interaction field of H_u. In this case, the reversal of magnetisation occurs at $(-H_{sw} + H_u)$ or $(+H_{sw} + H_u)$. Therefore, the distributions of these fields, FORC diagrams, can be obtained as $\rho(H_{sw}, H_u) = \frac{1}{M_s}\frac{\partial^2 M(H, H_r)}{\partial H \partial H_r}$, where $H_{sw} = (H - H_r)/2$ and $H_u = (H + H_r)/2$. Figure 4 presents the FORC diagrams of the samples. One can see that H_u for A0 is widely distributed across the range of tens of kA/m. This result indicates the existence of significant interparticle interactions, although their details cannot be analysed based solely on FORC diagrams because positive and negative values of H_u are not associated with ferromagnetic and antiferromagnetic natures, respectively. As t increases, the width of the distribution of H_u narrows and eventually becomes negligible compared to the experimental resolution of 8 kA m^{-1} at $t = 20.8$ nm for A21. This result is reasonable because dipolar interactions weaken at larger distances, as stated above.

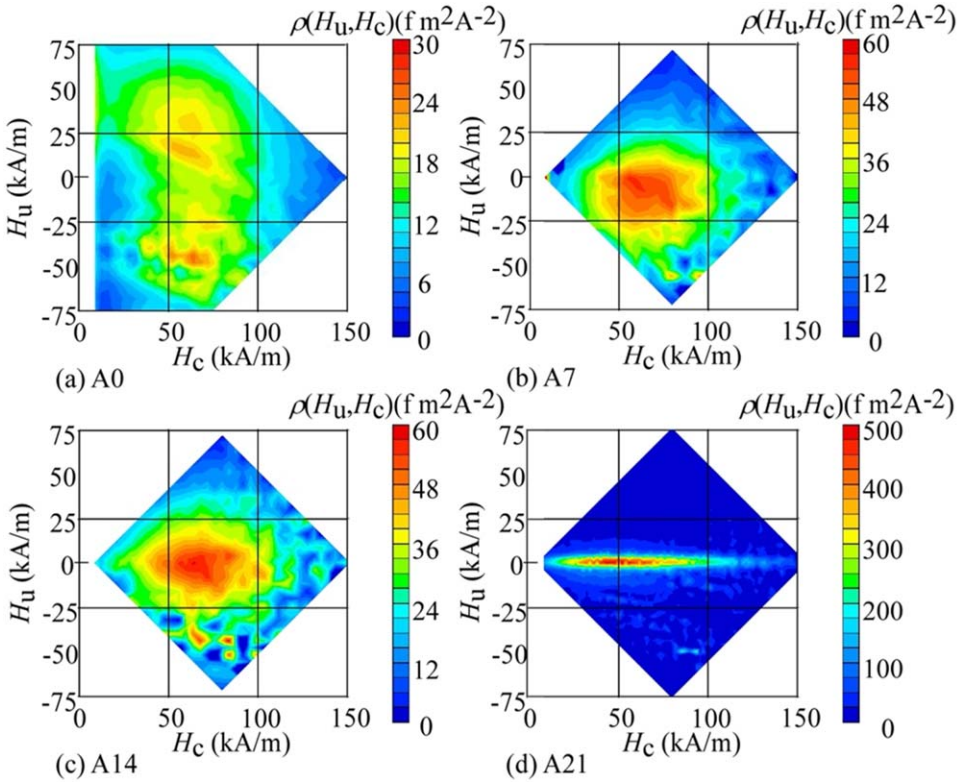

Figure 4. FORC diagrams of samples (a) A0, (b) A7, (c) A14, and (d) A21 at 2.0 K, where the contour maps show the probability distributions of the switching field of H_{sw} and interaction field of H_u.

At this stage, it should be noted that the width of the H_u distribution is much larger than the molecular field αM_s estimated from T_w for A0. It should also be noted that the molecular field represents the mean value of all magnetic couplings. Therefore, we can say that ferromagnetic-like and antiferromagnetic-like couplings coexist in almost equal quantities and cancel each other because the average magnetic interaction estimated from the Weiss temperature is much smaller than the distribution width of local interaction fields in the FORC diagrams. This result is consistent with a simple theoretical consideration. The dipolar magnetic field operates in a ferromagnetic-like manner on the neighbouring $\boldsymbol{\mu}$ in the axial direction of the source $\boldsymbol{\mu}$, whereas it operates in an antiferromagnetic-like manner on $\boldsymbol{\mu}$ in the equatorial direction. The faraway dipolar fields from a distant $\boldsymbol{\mu}$ are cancelled by demagnetising fields when the shape of the boundary between a neighbouring and distant $\boldsymbol{\mu}$ is set to be the same as the outward form of the powder sample. This interpretation based on small molecular fields is supported by the additional information acquired from the observed FORC diagrams, which lack wishbone-shaped ridges caused by the molecular fields from a distant $\boldsymbol{\mu}$ [15], as shown in figure 4.

The actual phenomena may be relatively complicated because the width of the distribution of H_u is evidently larger than the dipolar field from the single nearest neighboring $\boldsymbol{\mu}$. This field was calculated to be 13.5, 1.4, 0.3, and 0.1 kA/m for A0, A7, A14, and A21, respectively, using the aforementioned equation of $\frac{\mu_0 \mu^2}{2\pi r^3}$. In other words, H_u is cooperatively generated by multiple nanoparticles. This interpretation agrees with the spin-glass model, where the competition of ferromagnetic and antiferromagnetic interactions causes cooperative freezing of thermal fluctuations at the temperature corresponding not to T_w but to the distribution width of coupling strengths between different $\boldsymbol{\mu}$ [20]. We cannot discuss the nature of such superspin-glass-like behaviour further from the perspective of FORC diagrams because cooperative phenomena are entirely beyond the scope of application of the Preisach model [14, 15]. However, the coexistence of ferromagnetic and antiferromagnetic interactions is experimentally confirmed by currently comparing the results based on two conventional evaluation methods. This information is vital for advancing the study of superspin glasses.

4. Summary and prospects

Two conventional methods for evaluating interparticle magnetic interactions were applied to interparticle-distance-controlled magnetic nanoparticle assemblies. According to the Weiss temperatures of the superparamagnetic responses, the mean values of the interparticle magnetic interactions were relatively low compared to the blocking

temperature and seemed to be independent of the interparticle distance. In contrast, the interaction fields in the FORC diagrams were widely distributed for samples with narrow interparticle distances. However, the width of the interaction field distribution narrows with an increase in the non-magnetic layer thickness. Therefore, when comparing the small value of the mean field to larger local field effects, we can say that ferromagnetic-like and antiferromagnetic-like magnetic couplings are mixed in approximately equal quantities in nanoparticle assemblies, similar to atomic spin glasses. It should be noted that this evaluation could not be performed using only one of the two methods. For example, interparticle interactions may be misinterpreted as weak in all samples if only the Weiss temperature is considered. As demonstrated in this study, the complementary use of two methods is essential for characterising the magnetic interactions in nanoparticle assemblies.

Acknowledgments

This study was supported by JSPS KAKENHI Grant Number 19H04400 and JST-Mirai Program Grant Number JPMJMI18A3 in Japan. The authors would like to thank J Nishigaki and M Fukunaga for their technical assistance with sample synthesis.

Data availability statement

The data that support the findings of this study are available upon reasonable request from the authors.

ORCID iDs

H Mamiya https://orcid.org/0000-0002-7840-3008
J L Cuya Huaman https://orcid.org/0000-0001-9192-6877
K Suzuki https://orcid.org/0000-0002-9824-7620

References

[1] Hono K and Takahashi Y K 2016 L10-FePt granular films for heat-assisted magnetic recording media *Ultra-High-Density Magnetic Recording: Storage Materials and Media Designs* ed G Varvaro and F Casoli (Singapore: Jenny Stanford Publishing) pp 245–77
[2] Weddemann A *et al* 2010 Review and outlook: from single nanoparticles to self-assembled monolayers and granular GMR sensors *Beilstein J. Nanotechnol.* **1** 75–93
[3] Mamiya H 2013 Recent advances in understanding magnetic nanoparticles in AC magnetic fields and optimal design for targeted hyperthermia *J. Nanomater.* **2013** 752973
[4] Franco V, Blázquez J S, Ipus J J, Law J Y, Moreno-Ramírez L M and Conde A 2018 Magnetocaloric effect: from materials research to refrigeration devices *Prog. Mater Sci.* **93** 112–232
[5] Bedanta S and Kleemann W 2008 Supermagnetism *J. Phys. D: Appl. Phys.* **42** 013001
[6] Peddis D, Jönsson P E, Laureti S and Varvaro G 2014 Magnetic interactions: a tool to modify the magnetic properties of materials based on nanoparticles *Frontiers of Nanoscience* (Amsterdam, The Netherlands: Elsevier) pp 129–88
[7] Mamiya H, Nakatani I and Furubayashi T 1998 Blocking and freezing of magnetic moments for iron nitride fine particle systems *Phys. Rev. Lett.* **80** 177–80
[8] Mamiya H, Ohnuma M, Nakatani I and Furubayashi T 2004 Zero-field-cooled and field-cooled magnetization of individual nanomagnets and their assembly *Phys. Stat. Sol.* **A201** 3345–9
[9] Hiroi K, Komatsu K and Sato T 2011 Superspin glass originating from dipolar interaction with controlled interparticle distance among γ-Fe_2O_3 nanoparticles with silica shells *Phys. Rev.* B **83** 224423
[10] De Toro J A *et al* 2013 Controlled close-packing of ferrimagnetic nanoparticles: an assessment of the role of interparticle superexchange versus dipolar interactions *J. Phys. Chem.* C **117** 10213–9
[11] Hiroi K, Kura H, Ogawa T, Takahashi M and Sato T 2014 Magnetic ordered states induced by interparticle magnetostatic interaction in α-Fe/Au mixed nanoparticle assembly *J. Phys. Condens. Matter* **26** 176001
[12] Landers J, Stromberg F, Darbandi M, Schöppner CH, Keune W and Wende H 2015 Correlation of superparamagnetic relaxation with magnetic dipole interaction in capped iron-oxide nanoparticles *J. Phys. Condens. Matter* **27** 026002
[13] Fabris F, Kun-Hua T, Ross C A and Nunes W C 2019 Influence of dipolar interactions on the magnetic properties of superparamagnetic particle systems *J. Appl. Phys.* **126** 173905
[14] Mayergoyz I D and Friedman G 1988 Identification problem for 3D anisotropic preisach model of vector hysteresis *IEEE Trans. Mag.* **24** 2928–30
[15] Pike C R, Roberts A P and Verosub K L 1999 Characterizing interactions in fine magnetic particle systems using first order reversal curves *J. Appl. Phys.* **85** 6660–7
[16] Toro D *et al* 2017 Remanence plots as a probe of spin disorder in magnetic nanoparticles *Chem. Mater.* **29** 8258–68
[17] Pacakova B, Kubickova S, Salas G, Mantlikova A, Marciello M, Morales M P, Niznansky D and Vejpravova J 2017 Internal structure of magnetic nanoparticle determines magnetic response *J. Nanoscale* **9** 5129–40
[18] Mamiya H, Fukumoto H, Cuya Huaman J L, Suzuki K, Miyamura H and Jeyadevan B 2020 Estimation of magnetic anisotropy of individual magnetite nanoparticles for magnetic hyperthermia *ACS Nano.* **14** 8421–32
[19] Ding H L, Zhang Y X, Shihua W, Xu J M, Shicai X and Li G H 2012 Fe_3O_4@SiO_2 Core/Shell nanoparticles: the silica coating regulations with a single core for different core sizes and shell thicknesses *Chem. Mater.* **24** 4572–80
[20] Fischer K H and Hertz J A 1993 *Spin Glasses* (Cambridge: Cambridge University Press)